

1 Sources and export of particle-borne organic matter during a 2 monsoon flood in a catchment of northern Laos

3

4 E. Gourdin¹, S. Huon², O. Evrard¹, O. Ribolzi³, T. Bariac⁴, O. Sengtaheuanghoung⁵ and
5 S. Ayrault¹

6 [1]{Laboratoire des Sciences du Climat et de l'Environnement (LSCE), UMR 8212 (CEA-
7 CNRS-UVSQ-IPSL), Domaine du CNRS, avenue de la Terrasse, 91198 Gif-sur-Yvette cedex,
8 France}

9 [2]{Université Pierre et Marie Curie (UPMC), UMR 7618 iEES (UPMC-CNRS-IRD-INRA-
10 Université Paris 7-UPEC), case 120, 4 place Jussieu. 75252 Paris cedex 05, France}

11 [3]{IRD, Géosciences Environnement Toulouse (GET), UMR 5563 (CNRS-UPS-IRD), 14
12 avenue Edouard Belin, 31400 Toulouse, France}

13 [4]{CNRS, UMR 7618 iEES (UPMC-CNRS-IRD-INRA-Université Paris 7-UPEC), campus
14 INRA - AgroParisTech, Bâtiment EGER, 78550 Thiverval – Grignon, France}

15 [5]{Department of Agriculture Land Management (DALam), P.O. Box 4199, Ban
16 Nongviengkham, Xaythany District, Vientiane, Lao PDR}

17 Correspondence to: E. Gourdin (elian.gourdin@lsce.ipsl.fr)

18

19 **Abstract:**

20 Tropical rivers of Southeast Asia yields supply large quantities of carbon to the ocean. The
21 origin and dynamics of particulate organic matter were studied in the Houay Xon River
22 catchment located in northern Laos during the first erosive flood of the rainy season in May
23 2012. This cultivated catchment is equipped with three successive gauging stations draining
24 areas ranging between 0.2 and 11.6 km² on the main stem of the permanent stream, and two
25 additional stations draining 0.6 ha hillslopes. In addition, the sequential monitoring of
26 rainwater, overland flow and suspended organic matter compositions was conducted at the 1-
27 m² plot scale during a storm. The composition of particulate organic matter (total organic
28 carbon and total nitrogen concentrations, $\delta^{13}\text{C}$ and $\delta^{15}\text{N}$) was determined for suspended
29 sediment, soil surface (top 2 cm) and soil subsurface (gullies and riverbanks) samples
30 collected in the catchment (n = 57, 65 and 11, respectively). Hydrograph separation of event

1 water was achieved using water electric conductivity and $\delta^{18}\text{O}$ measurements for rainfall,
2 overland flow and river water base flow ($n = 9, 30$ and 57 , respectively). The composition of
3 particulate organic matter indicates that upstream suspended sediments mainly originated
4 from cultivated soils labelled by their C_3 vegetation cover (upland rice, fallow vegetation and
5 teak plantations). In contrast, channel banks characterized by C_4 vegetation (Napier grass)
6 supplied significant quantities of sediment to the river during the flood rising stage at the
7 upstream station as well as in downstream river sections. The highest runoff coefficient
8 (11.7%), sediment specific yield (433 kg ha^{-1}), total organic carbon specific yield (8.3 kgC ha^{-1})
9 and overland flow contribution (78-100%) were found downstream of reforested areas
10 planted with teaks. Swamps located along the main stream acted as sediment filters and
11 controlled the composition of suspended organic matter. Total organic carbon specific yields
12 were particularly high because they occurred during the first erosive storm of the rainy
13 season, just after the period of slash-and-burn operations in the catchment.

14

15 **1 Introduction**

16 Soil is a larger terrestrial reservoir of carbon than the biosphere and atmosphere combined
17 (e.g., Sarmiento and Gruber, 2002). Although tropical soils account for *ca.* 30% of the total
18 carbon storage (e.g., Dixon et al., 1994; Zech et al., 1997), high intensity storms (e.g.,
19 Goldsmith et al., 2008, Thothong et al., 2011) as well as deforestation and land use change are
20 responsible for high soil carbon losses and deliveries to rivers. Deforestation in Laos was
21 estimated to release *ca.* $85 \times 10^{12} \text{ gC yr}^{-1}$ to the atmosphere from 1979 to 1989 (Houghton,
22 1991). Degens et al. (1991) identified the Asian tropical rivers (e.g., Mekong,
23 Indus/Ganges/Brahmaputra) as the main contributors of dissolved (*ca.* $94 \times 10^{12} \text{ gC yr}^{-1}$) and
24 particulate (*ca.* $128 \times 10^{12} \text{ gC yr}^{-1}$) organic matter to the oceans, by delivering more than 50%
25 of global organic carbon inputs (about $335 \times 10^{12} \text{ gC yr}^{-1}$ excluding Australia). More recently,
26 Huang et al. (2012) estimated that tropical rivers of Asia have the highest specific total,
27 inorganic and organic, dissolved and particulate carbon yield in which *ca.* 25% of the delivery
28 occurs as particulate organic matter (POM). This latter component does not vary linearly with
29 total suspended sediment load (Ludwig et al., 1996), indicating that particulate organic matter
30 is associated with higher concentrations of mineral matter in high TSS loads that are supplied
31 to the rivers through erosion and sediment remobilization processes. Small mountainous
32 headwater catchments play a key role in the delivery pattern because they are characterized by
33 high specific discharges and sediment loads (Milliman and Syvitski, 1992). In this context,

1 processes that control organic matter export from tropical catchments should be better
2 understood and quantified, as they contribute significantly to drawdown or emission of carbon
3 dioxide (Lal, 2003).

4 Tropical storms may also result in the supply of large quantities of suspended sediment to
5 streams (Descroix et al., 2008; Evrard et al., 2010) and lead to numerous problems
6 downstream (Syvitski et al., 2005). Sediments can accumulate behind dams, which results in
7 the siltation of water reservoirs (Downing et al., 2008; Thothong et al., 2011). Suspended
8 organic matter also contributes to water quality degradation (Tanik et al., 1999) and plays a
9 major role in nutrient biogeochemical cycles (Quinton et al., 2010). It also constitutes a
10 potential vector for various contaminants such as metals, polycyclic aromatic hydrocarbons or
11 faecal bacteria (Ribolzi et al., 2010; Gateuille et al., 2014). In order to reduce the extent of
12 these negative impacts, sediment delivery by rivers needs to be monitored and controlled. The
13 design and implementation of appropriate management procedures require the identification
14 of the processes that mobilise organic matter from soils and export suspended organic matter
15 to rivers. To this end, total organic carbon (TOC) concentration measurements as well as
16 natural $^{15}\text{N}/^{14}\text{N}$ (e.g., Mariotti et al., 1983; Kao and Liu, 2000; Huon et al., 2006) and $^{13}\text{C}/^{12}\text{C}$
17 (e.g., Masiello and Druffel, 2001; Hilton et al., 2010; Smith et al., 2013) stable isotope
18 fingerprinting methods may be applied to particulate material collected from hillslopes to
19 rivers, either independently or in combination with fallout radionuclides to document
20 variations in sediment sources and pathways across catchments (e.g., Ritchie and McCarty,
21 2003; Ellis et al., 2012; Schindler Wildhaber et al., 2012; Ben Slimane et al., 2013; Koiter et
22 al., 2013). In addition, complementary information on sediment conveyed to the river by
23 runoff and overland flow can also be inferred from water tracers such as ^{18}O natural
24 abundance (for a review see Klaus and McDonnell, 2013).

25 In this study, rainwater, stream water, overland flow and suspended sediment were sampled in
26 the partly cultivated headwater catchment of the Houay Xon River, a small tributary of the
27 Mekong River in Laos, during an erosive flood event that occurred at the beginning of the
28 2012 rainy season. The aim was to: (1) estimate the overland flow contribution to stream
29 water and investigate its role during soil organic matter export, and (2) discriminate the
30 respective contributions of soil and stream channel sediment in order to identify the main
31 processes responsible for particulate organic matter delivery in nested catchments. This study
32 builds on previous research that provided a quantification of sediment dynamics during the
33 same flood. Gourdin et al. (2014), using fallout radionuclide measurements to quantify the
34 contributions of soil and stream channel sources to river.

1

2 **2 Study site**

3 The Houay Pano catchment is located 10 km south of Luang Prabang in northern Laos
4 (19.84°N - 102.14°E; **Fig. 1**). This catchment is part of the Monitoring Soil Erosion
5 Consortium (MSEC) network since 1998 (Valentin et al., 2008).

6 **[Fig. 1]**

7 The tropical monsoon climate of the region is characterized by the succession of dry and wet
8 seasons. Almost 80% of annual rainfall (1960-2013 average: 1302 ± 364 mm yr⁻¹) occurs
9 during the rainy season, from May to October (Ribolzi et al., 2008). The Houay Pano
10 permanent stream has an average base flow of 0.4 ± 0.1 L s⁻¹ and is equipped with 5 gauging
11 stations that subdivide the catchment into nested sub-catchments. Two of these stations, S1
12 and S4, draining 20 ha and 60 ha respectively, are located along the main stem of the stream.
13 Two additional stations (S7 and S8) draining two hillslopes (0.6 ha each) connected to the
14 main stream between S1 and S4 were also monitored. Between S1 and S4, water flows
15 through a swamp (0.19 ha), which is fed by groundwater (**Fig. 1**). Only temporary foot slope
16 and flood deposits can be found along the narrow section of the stream and the swamp
17 represents the main sediment accumulation zone in the upper catchment. The Houay Pano
18 stream flows into the Houay Xon River (22.4 km² catchment) and then across another swamp
19 (*ca.* 3 ha), partly occupied by fishponds (*ca.* 0.6 ha) at the outlet of the village. Stream
20 discharge is continuously monitored at S10 (draining a 11.6 km² sub-catchment), located 2.8
21 km downstream of S4. The Houay Xon is a tributary of the Nam Dong that flows into the
22 Mekong River in Luang Prabang City (Ribolzi et al., 2010). Sediment connectivity between
23 hillslopes and river is much lower in this downstream section, and most sediment therefore
24 deposits on footslopes before reaching the river. The drainage basin that includes the highest
25 elevations of the catchment is covered with old protected forests but no major tributary flows
26 into the Houay Xon River (**Fig. 1**). Ephemeral left bank streams located upstream of S10 did
27 not flow during the 23 May 2012 flood.

28 The geological basement of the Houay Pano upper catchment is mainly composed of pelites,
29 sandstones and greywackes (not sampled), overlaid in its uppermost NE part by
30 Carboniferous - Permian limestone cliffs (not sampled) that only cover a very small area in
31 the catchment. Except for the limestone cliffs and some sections of the narrow streambed,
32 soils or flooded soils of the swamps cover the entire catchment. They consist of deep (>2 m)

1 and moderately deep (>0.5 m) Alfisols (UNESCO, 1974), except along crests and ridges
2 where Inceptisols can be found (Chaplot et al., 2009). The soils have low pH ranging between
3 4.4 and 5.5 (Chaplot et al., 2009) indicating that carbonate precipitation does not occur in
4 soils and that they are therefore unlikely to supply particulate inorganic carbon to rivers.
5 Native vegetation consisted of lowland forest dominated by bamboos that were first cleared to
6 implement shifting cultivation of upland rice at the end of the 1960s (Huon et al., 2013).
7 Elevation across the Houay Xon catchment ranges between 272 and 1300 m a.s.l. Steep
8 hillslopes ($2-57^\circ$) are cultivated and are therefore very sensitive to soil erosion (Chaplot et al.,
9 2005; Ribolzi et al., 2011). Due to the decline of soil productivity triggered by soil erosion
10 over the years (Patin et al., 2012) and to an increasing labour need to control weed invasion
11 (Dupin et al., 2009), farmers progressively replaced rice fields with teak plantations in the
12 catchment (**Fig. 1**). In 2012 the Houay Pano catchment was covered by teaks (36%), rotating
13 cropping lands under fallow (35%), Job's tears (10%), bananas (4%), upland rice (3%) and
14 secondary forest ($<9\%$). The vegetation cover was different in the larger area drained by the
15 Houay Xon River, with 56% of forests, 15% under teak plantations and 23% croplands.

16

17 **3 Materials and methods**

18 **3.1 Sample and data collection**

19 Rainfall, stream and overland flow waters were sampled during a flood on 23 May 2012.
20 Rainfall intensity (I) was monitored with an automatic weather station (elevation: 536 m a.s.l.;
21 **Fig. 1**) and stream discharge was calculated from water level continuous records and rating
22 curves. Estimates of event water discharge (EWD), defined here as the total water volume
23 exported from each sub-catchment during the event minus the base flow discharge, were
24 calculated by adding sequential water volumes corresponding to the average discharge
25 between two successive water level measurements. Specific runoff (SR, in mm) was obtained
26 by dividing EWD by the corresponding sub-catchment area (Chow et al., 1988).

27 Rainfall was sampled with three cumulative collectors located: in the village near the
28 confluence between the Houay Pano and Houay Xon streams, near a teak plantation on the
29 hillslopes located just upstream of the village and within the upstream Houay Pano catchment
30 (**Fig. 1**). The runoff coefficient (RC) corresponds to the fraction of total rainfall that was
31 exported from the catchment during the event. Overland flow was collected at the outlet of 1-
32 m^2 experimental plot (OF_{1m^2}) during a storm on June 1, 2012 (**Fig. 2**; Patin et al., 2012).

1 Rainwater was collected in a nearby *ca.* 8-m² container. The experiment was conducted on a
2 soil with 18° slope and *ca.* 60% fallow vegetation cover (*ca.* 10 cm high; **Fig. 2a**). The rain
3 collector was installed at 1.8 m above soil surface to avoid splash contamination. Four
4 samples were collected in the top 3 cm of a soil profile (0-5 mm; 6-10 mm; 11-20 mm; 21-30
5 mm) within a *ca.* 400-cm² area adjacent to the experimental plot to measure the composition
6 of organic matter in the topsoil layer (**Fig. 2b**).

7 **[Fig. 2]**

8 River water was collected in 0.65 L polyethylene bottles for each 20-mm water level change
9 by automatic samplers installed at each gauging station. Sixty-nine total suspended sediment
10 (TSS) samples were collected at five stations, S1, S4 and S10 on the main stem and S7 - S8
11 for hillslopes drained by ephemeral tributaries (**Fig. 1**). Shortly after collection, all samples
12 were dried in 1 L aluminium trays in a gas oven (*ca.* 60-80°C) for 12-48 h. Preliminary
13 studies carried out in 2002-2007 showed that dissolved organic carbon concentrations in the
14 Houay Pano stream water are low, $1.8 \pm 0.4 \text{ mg L}^{-1}$ ($n = 74$) and $2.0 \pm 0.7 \text{ mg L}^{-1}$ ($n = 65$),
15 during base flow and peak discharge, respectively. With high-suspended sediment loads (see
16 further in the Results section), a 3 mgC L^{-1} content for dissolved organic matter would
17 represent 1-10 wt% of the total (dissolved and particulate) organic carbon load. On average,
18 $97 \pm 3 \%$ of the total organic matter recovered during the flood was particulate. Our results
19 are therefore very likely to reflect the composition and behaviour of particle-bound organic
20 matter, as the dissolved fraction was negligible. To expand the topsoil dataset available for the
21 catchment (Huon et al., 2013), additional soil cores were collected on hillslopes connected to
22 the Houay Pano stream and the Houay Xon River (**Fig. 1**) in May and December 2012.
23 Several gully ($n = 5$) and riverbank ($n = 6$) samples were also collected in December 2012 to
24 document the characteristics of the potential subsurface sources of sediment to the river.

25 Cumulated suspended sediment yields (SSY) were calculated at each station by summing the
26 total suspended sediment (TSS) exports between successive samples. The TSS concentration
27 was considered to vary linearly between successive measurements. Specific sediment yields
28 (S_Y) were calculated by dividing the cumulated SSY by the corresponding drainage area.

29 **3.2 Particulate organic matter composition measurements**

30 All samples were finely ground with an agate mortar, weighed and packed into tin capsules (5
31 x 9 mm) for analysis. Total organic carbon (TOC) and total nitrogen (TN) concentrations, and
32 ¹³C/¹²C and ¹⁵N/¹⁴N stable isotopes were measured using the Elementar® VarioPyro cube

1 analyzer on line with a Micromass[®] Isoprime Isotope Ratio Mass Spectrometer (IRMS)
2 facility (IEES, Paris). Analytical precision was better than $\pm 0.2 - 0.3\text{‰}$ vs. PDB-AIR
3 standards (Coplen et al., 1983) and 0.1 mg g^{-1} (equivalent to 0.01 wt.%) for $\delta^{13}\text{C}$ - $\delta^{15}\text{N}$ and
4 TOC-TN, respectively. Data reproducibility was checked by conducting replicate analyses of
5 a 99% pure tyrosine laboratory standard (Girardin and Mariotti, 1991) using 18 tyrosines per
6 batch of 50 samples. Analysis of a selection of samples was repeated and did not show any
7 variation in the measurements. The presence of carbonate minerals and carbonate rock
8 fragments in the samples was excluded after performing a test using a 30% HCl solution (no
9 CO₂ bubbling). For the entire flood, total particulate organic carbon yields (C_{SSY}) were
10 calculated by summing the successive TOC contents associated with suspended sediments
11 (SSY multiplied by TOC concentration). The TOC concentration of particulate organic matter
12 was assumed to vary linearly between successive samples. Specific TOC yields (C_Y) were
13 calculated by dividing the cumulated C_{SSY} by the corresponding drainage area.

14 **3.3 Water $\delta^{18}\text{O}$ and electrical conductivity measurements**

15 Water aliquots were recovered in 30-mL glass flasks from stream, overland flow and rain
16 samples (see **section 3.1** for details) and filtered using $<0.2 \mu\text{m}$ acetate filters. Stable $^{18}\text{O}/^{16}\text{O}$
17 isotope measurements were carried out using the standard CO₂ equilibration method (Epstein
18 and Mayeda, 1953) and determined with a VG Optima[®] mass spectrometer (IEES, Thiverval-
19 Grignon). Isotopic ratios are reported using the $\delta^{18}\text{O}$ notation, relative to the Vienna-Standard
20 Mean Ocean Water (V-SMOW; Gonfiantini, 1978) with an analytical precision better than \pm
21 0.1‰ . Water electrical conductivity (EC) was measured every 6-min at the inlet of each
22 gauging station using Schlumberger in situ CTD probes. Additional measurements were
23 conducted using an YSI[®] 556 probe for manually collected samples. Hydrograph separation
24 was obtained by applying end-member mixing equations using water electrical conductivity
25 and $\delta^{18}\text{O}$ measurements (Sklash and Farvolden, 1979; Ribolzi et al., 2000; Ladouche et al.,
26 2001).

27

1 4 Results

2 4.1 Composition of the potential sources of particulate organic matter in the 3 catchment

4 The mean organic matter characteristics are reported in **Table 1** for surface soils, gullies and
5 stream banks collected in the catchment, together with ^{137}Cs activities determined on the same
6 sample aliquots (Huon et al., 2013; Gourdin et al., 2014). High ^{137}Cs activities are measured
7 in surface soil samples, whereas gully and riverbank sites are depleted in this radioisotope
8 (**Table 1**).

9 [**Table 1**]

10 Surface (soils) and subsurface (channel banks and gullies) sources of particulate organic
11 matter are best discriminated by their TOC content that is significantly higher in surface soils.
12 The dominance of C_3 photosynthetic pathway plants across the catchment is reflected by low
13 $\delta^{13}\text{C}$ values in soils ($-25.5 \pm 1.4\%$). However, soil-originating particles accumulated in
14 sediments of the swamp provide ^{13}C -enriched compositions, up to *ca.* -15% , that are
15 explained by the input of organic matter derived from C_4 photosynthetic pathway plant
16 tissues. The C_4 plants found in the catchment are mainly Napier grasses growing in the
17 swamp and along some sections of the stream channel, and to a much lower extent, Job's tears
18 and maize cultivated on nearby hillslopes (Huon et al., 2013). Soil surface and subsurface
19 sources can also be distinguished by their $\delta^{15}\text{N}$ values that are slightly lower for the former
20 (**Table 1**). The results reflect high $^{15}\text{N}/^{14}\text{N}$ fractionation during incorporation and
21 mineralization of plant tissues in soils, which is typical in tropical environments (e.g.,
22 Amundson et al., 2003).

23 4.2 Monitoring water and particulate organic matter export at the microplot scale 24 during a rainfall event

25 The distribution of organic matter composition with soil depth is displayed on **Fig. 2b**. The
26 TOC content decreases exponentially with depth together with TN (not plotted), leading to a
27 nearly constant TOC : TN ratio of *ca.* 10 (**Fig. 2b**). Both $\delta^{13}\text{C}$ and $\delta^{15}\text{N}$ increase with soil
28 depth from -26.3 to -24.7% and from 6.6 to 8.6% , respectively, reflecting the contribution of
29 fallow vegetation debris depleted in ^{13}C and ^{15}N with respect to soil organic matter (Balesdent
30 et al., 1993). Overland flow samples (OF) were collected continuously at the outlet of the
31 experimental plot during the June 1st storm that lasted for 45-min. Cumulated rainfall was *ca.*

1 11 mm and its intensity reached 30 mm h⁻¹ during 20 min. Suspended sediment concentration
2 increased to a maximum of 4.7 g L⁻¹ (**Fig. 2c-d**). The estimated runoff coefficient was 77%
3 during the entire storm with an average infiltration rate of 3.3 mm h⁻¹, assuming no
4 evaporation during rainfall. As shown on **Fig. 2c**, suspended sediments exported from the
5 experimental plot were characterized by TOC, TOC/TN, δ¹³C and δ¹⁵N values that match
6 topsoil organic matter composition (**Fig. 2b**), with a slight evolution towards the composition
7 of deeper superficial layers (1-3 cm) at the end of the event. The higher TOC and lower δ¹³C
8 and δ¹⁵N values recorded at the beginning of the storm likely result from the preferential
9 export of fine soil organic matter. Similar behaviours were reported by Clark et al. (2013) in
10 the tropical Andes. They were associated with a greater contribution of non-fossil POC during
11 the rising stage and the peak discharge. In contrast, in the Swiss Alps, the initial decrease of
12 POC during the rising stage was assumed to result from in-channel clearing (Smith et al.,
13 2013). The evolution of rainwater and OF-δ¹⁸O is shown on **Fig. 2d**. At the beginning of the
14 storm, both parameters displayed a similar decreasing δ¹⁸O trend (from -3.8 to -5.5‰) with
15 increasing rainfall intensity, concomitant to a rise of the suspended load. Overland flow EC
16 averaged 20 ± 6 μS cm⁻¹ (range: 15 - 36 μS cm⁻¹, n = 17). The values are consistent with the
17 ones of two other cumulated OF samples (21 and 43 μS cm⁻¹) collected in the Houay Pano
18 catchment during the 23 May 2012 event (see **section 4.3**). Contrasted increasing trends were
19 also observed for rain- and OF-¹⁸O contents (reaching -1.7‰ and -4.0‰, respectively) during
20 the falling water stage. They reflected the mixing of progressively ¹⁸O-enriched rainwater
21 with former ¹⁸O-depleted rainwater temporarily stored in the topsoil. It is likely that OF that
22 triggers soil erosion and suspended sediment export better reflects the contribution of event
23 water to the stream than rainfall.

24 **4.3 Hydro-sedimentary characteristics of the 23 May 2012 flood**

25 This flood was triggered by a 48 min storm that brought 27 mm of cumulated rainfall between
26 11:36 am and 12:24 pm. According to Bricquet et al. (2003), this event has a return period of
27 *ca.* 0.01 year (34.7 mm day⁻¹). It was the first significant erosive event of the 2012 rainy
28 season and the first event with rainfall intensity exceeding 80 mm h⁻¹ (6-min time steps). The
29 main hydro-sedimentary characteristics of the flood are reported for the three gauging stations
30 in **Fig. 3 I-II-IIIa-b-c-d**.

31 **[Fig. 3]**

1 The lag time between stream discharge (Q) and rainfall intensity peaks differed at the three
2 stations. Q increased 10 min after the rainfall peak and reached its maximum 10 min later at
3 S1 (**Fig. 3Ia**), whereas both peaks were synchronous at S4 (**Fig. 3IIa**). Downstream, the lag
4 time between rainfall and Q peaks increased to 70 min at S10 (**Fig. 3IIIa**). The evolution of
5 TSS concentration that peaked at 24-47 g L⁻¹ (**Fig. 3I-II-IIIb**) displayed counterclockwise
6 hysteresis dynamics (Williams, 1989; Lenzi and Marchi, 2000) at the three stations. Even
7 though Q increased faster than TSS concentration at the beginning of the flood, water EC
8 decreased concomitantly at the three stations (**Fig. 3I-II-IIIc**). This behaviour suggests the
9 progressive mixing of pre-event water (i.e. groundwater) with a low TSS load by weakly
10 mineralized event water (i.e. overland flow) with high sediment loads, the proportion of the
11 latter increasing with decreasing EC. Pre-event EC values measured in the stream just before
12 the flood were 394, 320 and 450 $\mu\text{S cm}^{-1}$ at S1, S4 and S10, respectively (**Fig. 3I-II-IIIc**) and
13 strongly differed from the low values determined for OF (see above). As expected, the highest
14 values were recorded at S10, which is located downstream of riparian villages (Ribolzi et al.,
15 2010) where wastewaters characterized by high EC are directly released into the river. In
16 contrast, upstream of this village, stream waters exclusively originate from cultivated lands.
17 Pre-event water ¹⁸O content was estimated to -7.1‰ at station S4 with samples collected
18 before peak flow rise (**Fig. 3IId**). However, for S1 and S10, automatic sampling only took
19 place during the water rising stage and the composition of pre-event water had to be
20 estimated. At S1, a $\delta^{18}\text{O}$ value of -8‰ corresponding to a maximum EC of 394 $\mu\text{S cm}^{-1}$ was
21 estimated by fitting the correlative trend (see **section 5**). Pre-event and event waters could not
22 be distinguished with $\delta^{18}\text{O}$ signatures at S10. Overall, despite the limited number of samples
23 collected, the composition of cumulated rainwater remained rather constant in the catchment
24 (-5.1, -5.5 and -5.6‰), with an average of $-5.4 \pm 0.3\text{‰}$.

25 **4.4 Particulate organic matter export at catchment scales during the 23 May 2012** 26 **flood**

27 Large variations in suspended organic matter composition were recorded at S1 with TOC
28 concentration (20-70 mgC g⁻¹, **Fig. 3Ie**), TOC/TN (8-31, **Fig. 3If**), $\delta^{13}\text{C}$ (-26 to -15‰, **Fig.**
29 **3Ig**) and $\delta^{15}\text{N}$ (5.5-8.0‰, **Fig. 3Ih**) measurements. They all indicate changes in the source
30 delivering suspended organic matter to the river during the rising water stage. The $\delta^{13}\text{C}$
31 signature of suspended organic matter reach the average composition ($-25.5 \pm 1.4\text{‰}$; **Table 1**)
32 of topsoil organic matter in the catchment at peak flow and during the recession stage (**Fig.**

1 **3I-IIg**). Due to larger and more heterogeneous areas drained at S4 and S10, the temporal
2 evolution of TOC/TN, $\delta^{13}\text{C}$ and $\delta^{15}\text{N}$ in TSS (**Fig. 3II-III, e-f-g-h**) were less contrasted than at
3 S1. At S10, the mean TOC/TN was higher (17.0 ± 3.2) than at S1 (13.1 ± 5.9) and S4 ($10.3 \pm$
4 0.9), reflecting a greater contribution of vegetation debris and / or weakly mineralized organic
5 matter downstream than in upper parts of the catchment (**Table A1**). Furthermore, the highest
6 TOC/TN (23; **Fig. 3III f**) was obtained during the water peak discharge at S10 whereas it was
7 recorded at the beginning of the rising stage at S1 (31; **Fig. 3If**).

8

9 **5 Interpretation and discussion**

10 **5.1 Overland flow contribution to stream discharge**

11 **5.1.1 Evolution of water composition during the flood**

12 Water electrical conductivity and $\delta^{18}\text{O}$ measurements conducted on rainwater, overland flow
13 and stream water highlight in-channel mixing processes between base flow groundwater (pre-
14 event water) and event water characterized by contrasted signatures (**Fig. 4I**).

15 **[Fig. 4]**

16 At S1 (**Fig. 4Ia**), all samples are aligned between the PEW and OF_{1m^2} end-members during
17 both rising and recessing stages, suggesting that the composition of corresponding sources
18 remained constant during the event. This condition is one of the assumptions underpinning
19 hydrograph separation procedures (e.g. Buttle, 1994; Ribolzi et al., 2000; Klaus and
20 McDonnell, 2013). At S4 (**Fig. 4Ib**), the evolution of stream water composition during the
21 flood displays a more complex pattern, with the succession of three phases characterized by
22 distinct behaviours. During the rising stage, the trend between PEW and OF_{1m^2} is similar to
23 the situation observed at S1. Near peak flow, stream water EC and $\delta^{18}\text{O}$ concomitantly
24 decrease towards the signature of cumulated rainwater samples (**Fig. 4Ib**) until the dilution of
25 PEW by EW reaches its maximum. This behaviour likely reflects the progressive depletion of
26 rainwater in ^{18}O during the storm, as observed during the microplot experiment (**Fig. 2d**),
27 following a Rayleigh-type distillation process (Dansgaard, 1964). The decrease of EC in
28 stream water is also consistent with the supply of weakly mineralized overland flow water
29 mixing rainwater and pre-event soil water with low and high dissolved loads, respectively. A
30 remarkable point is that the water composition supplied by S7-S8 sub-catchments, referred to

1 as $OF_{0.6ha}$ (**Fig. 4Ib**), closely matches the composition of stream water during this period.
2 Finally, during the third phase corresponding to the recession period, the composition of the
3 river water evolved towards the “initial” PEW signature along a third mixing line. At S10,
4 stream water composition displayed large variations in EC but limited changes in $\delta^{18}O$ (range:
5 from -6.0 to -5.2‰, **Fig. 4Ic**). The EC values, decreasing from 450 to 155 $\mu S\ cm^{-1}$ at the
6 beginning of the event (**Fig. 3IIIc**), suggest a high contribution of OF at this station.

7 **5.1.2 Catchment hydrological characteristics inferred from hydrograph separation**

8 As highlighted by Klaus and McDonnell (2013), high-frequency analyses of rainfall and
9 runoff are necessary to record end-members intra-event signature variations and reduce
10 uncertainties associated with hydrograph separation. The microplot experiment recorded these
11 temporal variations during a single storm event (**Fig. 2d**). The OF signature displayed lower
12 variations (-5.5 to -3.7‰) than rainwater (-5.6 to -1.7‰) as a result of mixing between rain
13 and soil water. Although samples could not be taken during the 23 May 2012 flood, a similar
14 intra-storm evolution magnitude of *ca.* 2‰ for $OF-\delta^{18}O$ was assumed. In order to estimate
15 event water contribution to total water discharge monitored at each station, this possible intra-
16 storm variation of rainwater and overland flow signature must be taken into account
17 (McDonnell et al., 1990). The very close $\delta^{18}O$ values obtained for the three rainwater samples
18 collected on 23 May 2012 across the catchment remain consistent with the first assumption
19 formulated by Harris et al. (1995) regarding the spatial uniformity of cumulated rainwater
20 isotopic signature. However, the behaviour of stream water during peak discharge at S4 (**Fig.**
21 **3IIId-4Ib**) suggests the evolution of the OF end-member signature towards low $\delta^{18}O$ (as
22 recorded for $OF_{0.6ha}$ in **Fig. 4Ib**), consistent with a Rayleigh-type distillation of rainwater. Pre-
23 event soil water signature, likely enriched in ^{18}O by evaporation at the onset of the rainy
24 season (e.g., Hsieh et al., 1998), could not be characterized. Its higher $\delta^{18}O$ range can be
25 assumed to be responsible for the higher $\delta^{18}O$ observed for OF_{1m^2} during the 23 May 2012
26 flood (-3.9 to -2.5‰; **Fig. 4Ib**). The higher EC values recorded for $OF_{0.6ha}$ compared to OF_{1m^2}
27 likely result from the supply of dissolved elements by runoff because of interactions between
28 rainwater, vegetation, and soil particles along hillslopes. As the temporal evolution of
29 rainwater and of the resulting $OF-\delta^{18}O$ values could not be measured during the 23 May 2012
30 flood, we used EC only to provide estimates of overland flow contribution, taking into
31 account the potential variation of this end-member signature, from 20 to 150 $\mu S\ cm^{-1}$, during
32 the event (**Fig. 4II**).

1 **[Table 2]**

2 Estimates of event water discharge (EWD), specific runoff (SR) and runoff coefficient (RC)
3 are summarized in **Table 2**. Runoff coefficients are rather low in most parts of the catchment
4 (4.0 and 3.9% at S1 and S10, respectively), except at S4 where a higher value of 11.7% was
5 obtained (**Table 2**). Overall, those low runoff coefficients remained consistent with the high
6 infiltration rates reported by Patin et al. (2012) in soils of the same area ($>100 \text{ mm h}^{-1}$).
7 Chaplot and Poesen (2012) reported an annual runoff coefficient of *ca.* 13% for twelve 1-m²
8 plots monitored in this catchment. The values decrease in downstream direction, down to 6%
9 for S4 and 1.5% for S10. Estimates of the OF contribution to total water discharge, based on
10 the evolution of water EC, are displayed on **Fig. 4II**. At discharge peak, OF was lower at S1
11 (53-80%) than at S4 (78-100%) and S10 (67-95%). The highest value was obtained at S4
12 where the highest runoff coefficient was also recorded. This behaviour likely results from a
13 different soil cover in this sub-catchment where 32% of the surface is covered with teak,
14 compared to 14% and 15% upstream of S1 and S10, respectively. These teak plantations are
15 prone to soil erosion and characterized by low infiltration rates (Patin et al., 2012). Moreover,
16 the annual runoff coefficients reported by Chaplot and Poesen (2012) at S4 and S10 were
17 lower than those calculated in this study, but they were measured when teak plantations
18 covered a much smaller surface area in the catchment (2002-2003, Chaplot et al., 2005).
19 Overall, it is likely that teak plantations will enhance overland flow and soil erosion at least
20 during the years following their land use conversion.

21 **5.2 Particulate organic matter delivery during the 23 May 2012 flood**

22 **5.2.1 Sources of suspended organic matter in the catchment**

23 Variations in the composition of particulate organic matter reflect changes in the source
24 supplying suspended sediment in the catchment during the flood. For S1 and S4, this
25 evolution follows hyperbolic trends with suspended sediment loads for TOC, $\delta^{13}\text{C}$ and $\delta^{15}\text{N}$
26 and tends to reach the mean composition of catchment surface soils during the main transport
27 phase (**Fig. 5I-IIa-b**). As reported by Bellanger et al. (2004) in the Venezuelan Andes, this
28 behaviour indicates that sheet erosion was likely the dominant process. The composition of
29 suspended sediments in the study area is consistent with the supply of carbonate free soil-
30 detached particles exported from catchment's soils.

31 **[Fig. 5]**

1 However, Meybeck (1993) outlined that hyperbolic trends may indicate that a significant
2 fraction of particulate organic matter exported from mountainous regions by rivers may be
3 supplied by the direct erosion of sedimentary – metamorphic bedrocks (the so-called “fossil
4 carbon” pool) and pointed out that neglecting this source induces a bias in carbon budgets.
5 Fossil carbon may supply 90-100% of total particulate organic matter exported in rivers with
6 average annual suspended loads exceeding 5 g L^{-1} (Meybeck, 2006). In the Andes, Clark et al.
7 (2013) identified fossil POC contributions associated with TSS concentrations exceeding 1 g
8 L^{-1} . In a Taiwanese river, Hilton et al. (2011) reported suspended sediment concentrations up
9 to *ca.* 30 g L^{-1} with fossil POC concentrations up to *ca.* 0.1 g L^{-1} . Our results do not support
10 the hypothesis of a significant supply of rock-derived fossil carbon, which is often associated
11 with important sediment exports originating from gully systems (Duvert et al., 2010),
12 landslides and mass movements. These erosion processes were not observed in the Houay
13 Pano catchment during the study period. The few bedrock outcrops are not directly connected
14 to the stream. Moreover, the highest $\delta^{15}\text{N}$ values measured in suspended sediment samples
15 reflect the occurrence of soil derived organic matter rather than fossil organic matter (e.g.
16 Huon et al., 2006). The later should theoretically provide lower $\delta^{15}\text{N}$ values than the ones
17 found in soils. Preservation of organic matter in sedimentary and low-grade metamorphic
18 rocks takes place at “high temperature” (limited $^{15}\text{N}/^{14}\text{N}$ fractionation with respect to
19 vegetation) whereas incorporation and stabilization of organic matter in soils should occur at
20 “low surface temperature” (enhanced $^{15}\text{N}/^{14}\text{N}$ fractionation). Fossil particulate organic carbon
21 contributions have been identified using ^{14}C natural abundance and C-N stable isotope
22 measurements in various studies (e.g., Kao and Liu, 1997; Raymond and Bauer, 2001; Copard
23 et al., 2007; Graz et al., 2012; Smith et al., 2013). This approach could be applied to Houay
24 Pano samples in the future to further characterise the particulate organic matter. However, the
25 activities in ^{137}Cs that was supplied in the 1960s by atmospheric thermonuclear bomb fallout
26 (Ritchie and McHenry, 1990) measured in suspended sediments collected in Houay Pano and
27 Houay Xon Rivers remain in the same range as surface soil activities (above 1 Bq kg^{-1} ; **Table**
28 **1**; Gourdin et al., 2014). This result confirms that they may not originate from Paleozoic
29 bedrocks.

30 **5.2.2 Dynamics of suspended organic matter**

31 The ^{13}C -enriched compositions of material collected at S1 (**Fig. 5IIa**) first reflect the supply
32 of organic matter derived from C_4 photosynthetic pathway plants. Then, with increasing water
33 discharge, suspended sediments progressively incorporate ^{13}C -depleted organic matter

1 originating from soils covered by C₃ photosynthetic pathway plants that dominate in the
2 drainage area. Decreasing TOC/TN (increasing TN/TOC) and increasing $\delta^{15}\text{N}$ trends during
3 the flood are best explained by the re-suspension of weakly mineralized (low $\delta^{15}\text{N}$) C₄-plant
4 debris (high TOC/TN), followed by their mixing with soil organic matter exported from
5 cultivated fields and supplied by overland flow to the main stream (low TOC/TN, high $\delta^{15}\text{N}$).
6 A plot of $\delta^{13}\text{C}$ vs. TN/TOC shows that the composition of suspended sediment matches that of
7 the main pools of particulate organic matter in the catchment, i.e., surface soils and subsurface
8 soils (gullies and river banks, **Fig. 6**). Mixing between the two end-members is pictured by
9 linear relationships between both parameters for S1 and S10.

10 **[Fig. 6]**

11 Bedrock source compositions available from the literature for tropical catchments (i.e., Kao
12 and Liu, 2000, Hilton et al., 2010) fall outside the observed mixing trends. In addition, the
13 occurrence of light density charcoal fragments produced by slash-and-burn cultivation might
14 have slightly increased TOC/TN with respect to soil bulk organic matter (Soto et al., 1995;
15 Rumpel et al., 2006). Overland flow supply of particulate organic matter exported from soils
16 that are currently or were previously cultivated with upland rice is largely dominant at S4
17 compared to S1 (**Fig. 5I-IIa-b**). Fields cropped with C₄-plants only cover small areas in the
18 catchment and their imprint on soil organic matter composition is therefore limited (Huon et
19 al., 2013; de Rouw et al., 2015). The $\delta^{13}\text{C}$ recorded during and after the water discharge peak
20 were similar (-25.7‰; **Fig. 5IIa-b**) to those of surface soils, reflecting the dominance of
21 surface vs. subsurface sources in Houay Pano catchment. At S8, located close to S4 (**Fig. 1**),
22 $\delta^{15}\text{N}$ increased noticeably from 6.5 to 8.3‰ during the storm, indicating that ¹⁵N-depleted
23 organic matter (i.e., vegetation debris) was first exported and that erosion progressively
24 affected deeper ¹⁵N-enriched layers of the topsoil (**Table 1**). In contrast to the two other
25 stations, the maximum TOC/TN (23) recorded downstream at S10 occurred during the water
26 discharge peak (**Figs. 3III f and 5Ic**). Fresh organic matter characterized by high ratios is
27 exported with a time lag due to the remote location of its source (Gurnell, 2007). Suspended
28 organic matter transported at the beginning of the flood (range: from -23 to -21‰; **Table A1**,
29 **Fig. 5IIc**) is enriched in ¹³C and ¹⁵N compared to the mean surface soil and matches
30 subsurface soil signatures (stream banks and gullies, **Table 1**). This observation supports
31 previous findings showing the dominance of riverbank erosion characterized by the depletion
32 in fallout radionuclides measured for sediments collected at this station (Gourdin et al., 2014).
33 Positive correlative trends between soil TOC and ¹³⁷Cs inventories suggest that a similar

1 process, i.e. erosion and erosion-induced carbon depletion, controlled their concomitant
2 decrease since the onset of cultivation in the 1960's (Huon et al., 2013). Smith and Blake
3 (2014) reported similar correlations for riverine sediments in some of their study sites. We
4 could not derive any similar relationship during the 23 May 2012 flood (data not shown).

5 Contribution of overland flow to stream water discharge derived from hydrograph separation
6 can be linked to the source of suspended organic matter (**Fig. 5 III**) as well as to the extent of
7 particulate organic matter transfer (**Fig. 5 IV**). In terms of water - sediment dynamics, high
8 OF contributions (above *ca.* 50%) supply large quantities of soil organic matter, characterized
9 by lower TOC contents and enriched isotopic compositions compared to fresh vegetation
10 debris, to the river. In contrast, low OF contributions may indicate the dominance of
11 riverbank erosion and remobilization of sediment deposited on the riverbed during previous
12 floods. Based on hydrograph separation, it is then possible to draw sediment and particulate
13 organic carbon budgets at the catchment's scale in areas where surface soil erosion dominates.

14

15 **5.2.3 Suspended sediment and particulate organic carbon deliveries**

16 Total suspended sediment exports are summarized in **Table 3** for S1, S4 and S10 sub-
17 catchments.

18 **[Table 3]**

19 Compared to the annual sediment yield measured in 2002-2003 at S4 ($2090 \text{ kg ha}^{-1} \text{ yr}^{-1}$) and
20 S10 ($540 \text{ kg ha}^{-1} \text{ yr}^{-1}$) reported by Chaplot and Poesen (2012), the 23 May 2012 flood
21 represented *ca.* 21% of the total annual exports recorded at both stations. These deliveries are
22 high for a single rainfall event of moderate intensity. However, fallout radionuclide
23 measurements (Gourdin et al., 2014) indicate that this flood was the first important erosive
24 event of the 2012 rainy season and that it mainly exported remobilized river channel sediment
25 (*ca.* 80%). The TSS yield (S_Y) of *ca.* 433 kg ha^{-1} (8.3 kgC ha^{-1}) at S4 is greater than at S1 and
26 S10 (**Table 3**) and remains consistent with higher specific runoff and runoff coefficient values
27 recorded at this station (**Table 2**). Overall, we did not observe any decrease in specific carbon
28 delivery when the drainage area of catchments increased. This counter-intuitive result is likely
29 explained by the occurrence of a swamp along the main stream between S1 and S4. In the
30 upper part of the catchment, it acts like a filter for sediments conveyed during low to medium
31 magnitude floods (**Fig. 1**). In this swamp, Napier grass reduces stream flow velocity and
32 enhances particle deposition. About 33 Mg of soil-derived organic carbon was estimated to

1 have accumulated in this area since the early 1960's (Huon et al., 2013). This swamp therefore
2 played a key role by reducing downstream export of suspended sediment during the 23 May
3 2012 flood. It also explains why the high $\delta^{13}\text{C}$ values of TSS loads observed during the rising
4 water stage upstream of the swamp (at S1) are not found in sediments collected at S4. Soil-
5 derived organic matter supplied by overland flow supplied the major part of the TSS during
6 the rising stage, downstream of the swamp. A comparable role of sediment filter can be
7 attributed to the wetlands located at the outlet of the village. However, in contrast the latter
8 mainly supplied streambank material to the river. As they were covered by Napier grass, this
9 channel bank material was characterized by higher $\delta^{13}\text{C}$ values as measured at S10. The shift
10 in the POC signature thereby confirms the results obtained with radionuclide activity
11 measurements carried out on the same samples (Gourdin et al., 2014).

12

13 **6 Concluding remarks**

14 The composition of suspended organic matter and stream water was measured during the first
15 erosive flood of the 2012 rainy season in a cultivated catchment of northern Laos. These
16 measurements provided an efficient way to quantify the contribution of particulate organic
17 matter sources along a network of nested gauging stations.

18 Quantification of the overland flow contribution (rather than rainfall) with hydrological
19 tracers ($\delta^{18}\text{O}$ and electrical conductivity) strengthened the procedure used to identify the
20 sources of particulate organic matter in the catchment.

21 In the upper part of the drainage basin (Houay Pano sub-catchment), the composition of
22 suspended organic matter shows that sediment mainly originated from in-channel and nearby
23 sources during the rising stage and from cultivated topsoil during peak flow and flood
24 recessing stage.

25 Downstream, the composition of suspended organic matter in the Houay Xon River reflected
26 the dominant supply of subsurface sources (riverbanks and gullies) and a subsequent dilution
27 of soil-derived organic matter delivery by channel - bank mixing and mobilization processes.

28 Wetlands and swamps played a key role by trapping sediment in the upstream and steeper part
29 of the catchment and by remobilizing riverbank deposits further downstream.

30 Overall, the specific particulate organic matter delivery estimated at the catchment outlet was
31 rather high for a flood of moderate magnitude, and this result was attributed to its occurrence
32 at the onset of the rainy season, after field clearing by slash-and-burn operations.

1

2 **Acknowledgements**

3 The authors would like to thank the Lao NAFRI (National Agriculture and Forestry Research
4 Institute in Vientiane) and the MSEC project (Multi-Scale Environment Changes) for their
5 support. They are also grateful to Keo Oudone Latsachack, Bounsamai Soulileuth and
6 Chanthamousone Thammahacksa for their help in the field, to Véronique Vaury (iEES-Paris)
7 for organic matter composition measurements, and to Patricia Richard (iEES-Thiverval
8 Grignon) for $\delta^{18}\text{O}$ measurements of water samples. Elian Gourdin received a PhD fellowship
9 from Paris-Sud University, Orsay, France. This work received financial support from the
10 French CNRS EC2CO / BIOHEFECT program (Belcrue project). The authors are thankful for
11 the constructive comments of two anonymous referees who helped improving a former draft
12 of the manuscript.

13

1 **References**

- 2 Amundson, R., Austin, A. T., Schuur, E. A. G., Yoo, K., Matzek, V., Kendall, C., Uebersax,
3 A., Brenner, D. and Baisden, W. T.: Global patterns of the isotopic composition of soil and
4 plant nitrogen, *Global Biogeochemical Cycles*, 17(1), 1031, 2003.
- 5 Balesdent, J., Girardin, C. and Mariotti, A.: Site-related $\delta^{13}\text{C}$ of tree leaves and soil organic
6 matter in a temperate forest, *Ecology*, 74(6), 1713-1721, 1993.
- 7 Bellanger, B., Huon, S., Velasquez, F., Vallès, V., Girardin, C. and Mariotti, A.: Monitoring
8 soil organic carbon erosion with $\delta^{13}\text{C}$ and $\delta^{15}\text{N}$ on experimental field plots in the Venezuelan
9 Andes, *Catena*, 58(2), 125–150, 2004.
- 10 Ben Slimane, A., Raclot, D., Evrard, O., Sanaa, M., Lefèvre, I., Ahmadi, M., Tounsi, M.,
11 Rumpel, C., Ben Mammou, A. and Le Bissonnais, Y.: Fingerprinting sediment sources in the
12 outlet reservoir of a hilly cultivated catchment in Tunisia, *J. Soils Sediments*, 13(4), 801–815,
13 2013.
- 14 Bricquet, J.-P., Boonsaner, A., Bouahom, B. and Toan, T. D.: Statistical Analysis of Long
15 Series Rainfall Data: A Regional Study in South-East Asia, In A. R. Maglinao, C. Valentin, F.
16 Penning de Vries (Eds.), *From soil research to land and water management: harmonizing
17 people and nature: proceedings of the IWMI-ADB project annual meeting and 7th MSEC
18 assembly. Vientiane (LAO). (pp. 83–89). Vientiane (LAO): IWMI-ADB Project Annual
19 Meeting; MSEC Assembly, 7, 2003.*
- 20 Buttle, J.M.: Isotope hydrograph separations and rapid delivery of pre-event water from
21 drainage basins, *Prog. Phys. Geogr.*, 18, 16–41, 1994.
- 22 Chaplot, V. and Poesen, J.: Sediment, soil organic carbon and runoff delivery at various
23 spatial scales, *Catena*, 88, 46–56, 2012.
- 24 Chaplot, V, Coadoulebrozec, E., Silvera, N. and Valentin, C.: Spatial and temporal
25 assessment of linear erosion in catchments under sloping lands of northern Laos, *Catena*,
26 63(2-3), 167–184, 2005.
- 27 Chaplot, V., Podwojewski, P., Phachomphon, K. and Valentin, C.: Soil erosion impact on soil
28 organic carbon spatial variability on steep tropical slopes, *Soil Science Society of America
29 Journal*, 73(3), 769, 2009.
- 30 Chow, V.T., Maidment, D.R. and Mays, L.W.: *Applied Hydrology*, McGraw Hill Book Co.
31 572 p., 1988.

1 Clark, K. E., Hilton, R. G., West, A. J., Malhi, Y., Gröcke, D. R., Bryant, C. L., Ascough, P.
2 L., Robles Caceres, A. and New, M.: New views on “old” carbon in the Amazon River:
3 Insight from the source of organic carbon eroded from the Peruvian Andes, *Geochemistry,*
4 *Geophysics, Geosystems*, 14(5), 1644–1659, 2013.

5 Copard, Y., Amiotte-Suchet, P. and Di-Giovanni, C.: Storage and release of fossil organic
6 carbon related to weathering of sedimentary rocks, *Earth Planet. Sci. Lett.* 258, 345–357,
7 2007.

8 Coplen, T.B., Kendall, C. and Hopple, J.: Comparison of stable isotope reference samples.
9 *Nature*, 302, 236–238, 1983.

10 Dansgaard, W.: Stable isotopes in precipitation, *Tellus*, 16, 436–468, 1964.

11 Degens, E. T., Kempe, S. and Richey, J. E.: Summary: Biogeochemistry of major world
12 rivers, In E. T. Degens, S. Kempe and J. E. Richey (Eds.), *Biogeochemistry of major world*
13 *rivers*, SCOPE Rep. 42, John Wiley and Sons, Chichester, 323–347, 1991.

14 de Rouw, A., Soulileuth, B. and Huon, S.: Stable carbon isotope ratios in soil and vegetation
15 shift with cultivation, *Agriculture, Ecosystems and Environment*, 200, 161–168, 2015.

16 Descroix, L., González Barrios, J. L., Viramontes, D., Poulencard, J., Anaya, E., Esteves, M.
17 and Estrada, J.: Gully and sheet erosion on subtropical mountain slopes: Their respective roles
18 and the scale effect, *Catena*, 72(3), 325–339, 2008.

19 Dixon, R.K., Brown, S., Houghton, R.A., Solomon, A.M., Trexler, M.C. and Wisniewski, J.:
20 Carbon pools and flux of global forest ecosystems, *Science*, 263, 185–191, 1994.

21 Downing, J. A., Cole, J. J., Middelburg, J. J., Striegl, R. G., Duarte, C. M., Kortelainen, P.,
22 Prairie, Y. T. and Laube, K. A.: Sediment organic carbon burial in agriculturally eutrophic
23 impoundments over the last century, *Global Biogeochemical Cycles*, 22(1), 1–10, 2008.

24 Dupin, B., de Rouw, A., Phantahvong, K. B. and Valentin, C.: Assessment of tillage erosion
25 rates on steep slopes in northern Laos, *Soil and Tillage Research*, 103(1), 119–126, 2009.

26 Duvert, C., Gratiot, N., Evrard, O., Navratil, O., Némery, J., Prat, C. and Esteves, M.: Drivers
27 of erosion and suspended sediment transport in three headwater catchments of the Mexican
28 Central Highlands, *Geomorphology*, 123, 243–256, 2010.

29 Ellis, E. E., Keil, R. G., Ingalls, A. E., Richey, J. E. and Alin, S. R.: Seasonal variability in the
30 sources of particulate organic matter of the Mekong River as discerned by elemental and
31 lignin analyses, *J. Geophys. Res.*, 117, G01038, 2012.

- 1 Epstein, S. and Mayeda, T.: Variation of ^{18}O content of waters from natural sources,
2 *Geochimica et Cosmochimica Acta*, 4(5), 213–224, 1953.
- 3 Evrard, O., Némery, J., Gratiot, N., Duvert, C., Ayrault, S., Lefèvre, I., Poulenard, J., Prat, C.,
4 Bonté, P. and Esteves, M.: Sediment dynamics during the rainy season in tropical highland
5 catchments of central Mexico using fallout radionuclides, *Geomorphology*, 124, 42–54, 2010.
- 6 Gateuille, D., Evrard, O., Lefèvre, I., Moreau-Guigon, E., Alliot, F., Chevreuil, M. and
7 Mouchel, J.-M.: Mass balance and depollution times of Polycyclic Aromatic Hydrocarbons in
8 rural nested catchments of an early industrialized region (Orgeval River, Seine River basin,
9 France), *Science of the Total Environment*, 470-471, 608-617, 2014.
- 10 Girardin, C. and Mariotti, A.: Analyse isotopique du ^{13}C en abondance naturelle un système
11 automatique avec robot préparateur, *Cah. Orstom, sér. Pédol.*, vol. XXVI,(120), 371–380,
12 1991.
- 13 Goldsmith, S.T., Carey, A.E., Lyons, W.B., Kao, S.-J., Lee, T.-Y. and Chen, J.: Extreme
14 storm events, landscape denudation, and carbon sequestration: Typhoon Mindulle, Choshui
15 River, Taiwan, *Geology*, 36, 483–486, 2008.
- 16 Gonfiantini, R.: Standards for stable isotope measurements in natural compounds. *Nature*,
17 271(5645), 534–536, 1978.
- 18 Gourdin, E., Evrard, O., Huon, S., Lefèvre, I., Ribolzi, O., Reyss, J.-L., Sengtaheuanghoung
19 and O., Ayrault, S.: Suspended sediment dynamics in a Southeast Asian mountainous
20 catchment: combining river monitoring and fallout radionuclide tracers, *Journal of*
21 *Hydrology*, 519, 1811–1823, 2014.
- 22 Graz, Y., Di-Giovanni, C., Copard, Y., Mathys, N., Cras, A. and Marc, V.: Annual fossil
23 organic carbon delivery due to mechanical and chemical weathering of marly badlands areas,
24 *Earth Surf. Process. Landforms*, 37(12), 1263–1271, 2012.
- 25 Gurnell, A. M.: Analogies between mineral sediment and vegetative particle dynamics in
26 fluvial systems, *Geomorphology*, 89(1-2), 9–22, 2007.
- 27 Harris, D.M., McDonnell, J.J. and Rodhe, A.: Hydrograph separation using continuous open
28 system isotope mixing, *Water Resour. Res.* 31, 157–171, 1995.
- 29 Hilton, R.G., Galy, A., Hovius, N., Horng, M.-J. and Chen, H.: The isotopic composition of
30 particulate organic carbon in mountain rivers of Taiwan, *Geochimica et Cosmochimica Acta*,
31 74, 3164–3181, 2010.

- 1 Hilton, R.G., Galy, A., Hovius, N., Horng, M.-J. and Chen, H.: Efficient transport of fossil
2 organic carbon to the ocean by steep mountain rivers: An orogenic carbon sequestration
3 mechanism, *Geology*, 39(1), 71–74, 2011.
- 4 Houghton, R.A.: Tropical deforestation and atmospheric carbon dioxide, *Clim. Change*, 19,
5 99–118, 1991.
- 6 Hsieh, J. C. C., Chadwick, O. A., Kelly, E. F. and Savin, S.M.: Oxygen isotopic composition
7 of soil water: Quantifying evaporation and transpiration, *Geoderma*, 82, 269–293, 1998.
- 8 Huang, T.-H., Fu, Y.-H., Pan, P.-Y. and Chen, C.-T. A.: Fluvial carbon fluxes in tropical
9 rivers, *Curr. Opin. Environ. Sustain.* 4, 162–169, 2012.
- 10 Huon, S., Bellanger, B., Bonté, P., Sogon, S., Podwojewski, P., Girardin, C., Valentin, C., De
11 Rouw, A., Velasquez, F., Bricquet, J.-P. and Mariotti, A.: Monitoring soil organic carbon
12 erosion with isotopic tracers: two case studies on cultivated tropical catchments with steep
13 slopes (Laos, Venezuela), In Roose, E.; Lal, R.; Barthès, B.; Feller C.; Stewart, B. A. (Ed.),
14 *Advances in Soil Science. Soil erosion and carbon dynamics* (pp. 301–328.). CRC Press,
15 Boca Raton. Florida (USA), 2006.
- 16 Huon, S., de Rouw, A., Bonté, P., Robain, H., Valentin, C., Lefèvre, I., Girardin, C., Le
17 Troquer, Y., Podwojewski, P. and Sengtaheuanghoung O.: Long-term soil carbon loss and
18 accumulation in a catchment following the conversion of forest to arable land in northern
19 Laos, *Agriculture, Ecosystems and Environment*, 169, 43–57, 2013.
- 20 Kao, S.J. and Liu, K.K.: Fluxes of dissolved and nonfossil particulate organic carbon from an
21 Oceania small river (Lanyang Hsi) in Taiwan, *Biogeochemistry*, 39, 255–269, 1997.
- 22 Kao, S.J. and Liu, K.K.: Stable carbon and nitrogen isotope systematics in a human- disturbed
23 watershed (Lanyang-Hsi) in Taiwan and the estimation of biogenic particulate organic carbon
24 and nitrogen fluxes, *Global Biogeochemical Cycles*, 14(1), 189–198, 2000.
- 25 Klaus, J. and McDonnell, J.J.: Hydrograph separation using stable isotopes: Review and
26 evaluation, *Journal of Hydrology*, 505, 47–64, 2013.
- 27 Koiter, A. J., Owens, P. N., Petticrew, E. L. and Lobb, D. A.: The behavioural characteristics
28 of sediment properties and their implications for sediment fingerprinting as an approach for
29 identifying sediment sources in river basins, *Earth-Science Reviews*, 125, 24–42, 2013.

- 1 Ladouche, B., Probst, A., Viville, D., Idir, S., Baqué, D., Loubet, M., Probst, J.-L. and Bariac,
2 T.: Hydrograph separation using isotopic , chemical and hydrological approaches (Strengbach
3 catchment , France), *Journal of Hydrology*, 242, 255–274, 2001.
- 4 Lal, R.: Soil erosion and the global carbon budget, *Environ. Int.*, 29(4), 437–450, 2003.
- 5 Lenzi, M.A. and Marchi, L.: Suspended sediment load during floods in a small stream of the
6 Dolomites (Northeastern Italy), *Catena*, 39, 267-282, 2000.
- 7 Ludwig, W., Probst, J. and Kempe, S.: Predicting the oceanic input of organic carbon by
8 continental erosion, *Global Biogeochemical Cycles*, 10(1), 23–41, 1996.
- 9 Mariotti, A., Lancelot, C. and Billen, G.: Natural isotopic composition of nitrogen as a tracer
10 of origin for suspended organic matter in the Scheldt estuary, *Geochimica et Cosmochimica*
11 *Acta*, 48, 549–555, 1983.
- 12 Masiello, C.A. and Druffel, E.R.M.: Carbon isotope geochemistry of the Santa Clara River,
13 *Global Biogeochemical Cycles*, 15(2), 407–416, 2001.
- 14 McDonnell, J.J., Bonell, M., Stewart, M.K. and Pearce, A.J.: Deuterium variations in storm
15 rainfall: implications for stream hydrograph separation, *Water Resour. Res.*, 26, 455–458,
16 1990.
- 17 Meybeck, M.: Riverine transport of atmospheric carbon: sources, global typology and budget,
18 *Water. Air. Soil Pollut.*, 70, 443–463, 1993.
- 19 Meybeck, M.: Origins and behaviors of carbon species in world rivers, In Roose, E.; Lal, R.;
20 Barthès, B.; Feller C.; Stewart, B. A. (Ed.), *Soil erosion and Carbon Dynamics* (pp. 209–238).
21 CRC Press, Boca Raton. Florida (USA), 2006.
- 22 Milliman, J.D. and Syvitski, J.P.M.: Geomorphic / tectonic control of sediment discharge to
23 the ocean : the importance of small mountainous rivers, *J. Geol.*, 100, 525–544, 1992.
- 24 Patin, J., Mouche, E., Ribolzi, O., Chaplot, V., Sengtahevong, O., Latsachak, K. O.,
25 Soulileuth, B. and Valentin, C.: Analysis of runoff production at the plot scale during a long-
26 term survey of a small agricultural catchment in Lao PDR, *Journal of Hydrology*, 426-427,
27 79–92, 2012.
- 28 Quinton, J. N., Govers, G., Van Oost, K. and Bardgett, R. D.: The impact of agricultural soil
29 erosion on biogeochemical cycling, *Nature Geoscience*, 3(5), 311–314, 2010.
- 30 Raymond, P.A. and Bauer, J.E.: Riverine export of aged terrestrial organic matter to the North
31 Atlantic Ocean, *Nature*, 409, 497–500, 2001.

- 1 Ribolzi, O., Andrieux, P., Valles, V., Bouzigues, R., Bariac, T. and Voltz, M.: Contribution of
2 groundwater and overland flows to storm flow generation in a cultivated Mediterranean
3 catchment. Quantification by natural chemical tracing, *Journal of Hydrology*, 233, 241–257,
4 2000.
- 5 Ribolzi, O., Cuny, J., Sengsoulichanh, P., Pierret, A., Thiébaux, J. P., Huon, S., Bourdon, E.,
6 Robain, E. and Sengtaheuanghong O.: Assessment of water quality along a tributary of the
7 Mekong River in a mountainous, mixed land-use environment of the Lao P.D.R., *The Lao*
8 *Journal of Agriculture and Forestry*, (17), 91–111, 2008.
- 9 Ribolzi, O., Cuny, J., Sengsoulichanh, P., Mousquès, C., Soulileuth, B., Pierret, A., Huon, S.
10 and Sengtaheuanghong O.: Land use and water quality along a Mekong tributary in northern
11 Lao P.D.R., *Environmental management*, 47(2), 291–302, 2010.
- 12 Ribolzi, O., Patin, J., Bresson, L. M., Latsachack, K. O., Mouche, E., Sengtaheuanghong, O.,
13 Silvera, N., Thiébaux, J. P. and Valentin, C.: Impact of slope gradient on soil surface features
14 and infiltration on steep slopes in northern Laos, *Geomorphology*, 127, 53–63, 2011.
- 15 Ritchie, J.C. and McCarty, G.W.: ¹³⁷Cesium and soil carbon in a small agricultural watershed,
16 *Soil and Tillage Research*, 69, 45–51, 2003.
- 17 Ritchie, J. C. and McHenry, J. R.: Application of Radioactive Fallout Cesium-137 for
18 Measuring Soil Erosion and Sediment Accumulation Rates and Patterns: A Review, *J.*
19 *Environ. Qual.*, 19, 215–233, 1990.
- 20 Rumpel, C., Chaplot, V., Planchon, O., Bernadou, J., Valentin, C. and Mariotti, A.:
21 Preferential erosion of black carbon on steep slopes with slash and burn agriculture, *Catena*,
22 65(1), 30–40, 2006.
- 23 Sarmiento, J.L. and Gruber, N.: Sinks for anthropogenic carbon, *Physics Today*, 55, 30–36,
24 2002.
- 25 Schindler Wildhaber, Y., Liechti, R. and Alewell, C.: Organic matter dynamics and stable
26 isotope signature as tracers of the sources of suspended sediment, *Biogeosciences*, 9, 1985–
27 1996, 2012.
- 28 Sklash, M. G. and Farvolden, R. N.: The role of groundwater in storm runoff, *Journal of*
29 *Hydrology*, 43, 45–65, 1979.

- 1 Smith, H.G. and Blake, W.H.: Sediment fingerprinting in agricultural catchments: A critical
2 re-examination of source discrimination and data corrections, *Geomorphology*, 204, 177–191,
3 2014.
- 4 Smith, J.C., Galy, A., Hovius, N., Tye, A.M., Turowski, J.M. and Schleppe, P.: Runoff-driven
5 export of particulate organic carbon from soil in temperate forested uplands, *Earth Planet. Sci.*
6 *Lett.*, 365, 198–208, 2013.
- 7 Soto, B., Basanta, R., Perez, R. and Diaz-Fierros, F.: An experimental study of the influence
8 of traditional slash-and-burn practices on soil erosion, *Catena*, 24(1), 13–23, 1995.
- 9 Syvitski, J. P. M., Vörösmarty, C. J., Kettner, A. J. and Green, P.: Impact of humans on the
10 flux of terrestrial sediment to the global coastal ocean, *Science*, 308(5720), 376–80, 2005.
- 11 Tanik, A., Beler Baykal, B. and Gonenc, I. E.: The impact of agricultural pollutants in six
12 drinking water reservoirs, *Water Science and Technology*, 40(2), 11–17, 1999.
- 13 Thothong, W., Huon, S., Janeau, J.-L., Boonsaner, A., de Rouw, A., Planchon, O., Bardoux,
14 G. and Parkpian, P.: Impact of land use change and rainfall on sediment and carbon
15 accumulation in a water reservoir of North Thailand, *Agriculture, Ecosystems and*
16 *Environment*, 140(3-4), 521–533, 2011.
- 17 UNESCO (United Nations Educational Scientific and Cultural Organization): FAO/UNESCO
18 Soil map of the world, 1:5,000,000 Vol.1. Paris: UNESCO, 1974.
- 19 Valentin, C., Agus, F., Alamban, R., Boosaner, A., Bricquet, J. P., Chaplot, V., de Guzman,
20 T., de Rouw, A., Janeau, J.L., Orange, D., Phachomphonh, K., Podwojewski, P., Ribolzi, O.,
21 Silvera, N., Subagyono, K., Thiébaux, J.P. and Vadari, T.: Runoff and sediment losses from
22 27 upland catchments in Southeast Asia: Impact of rapid land use changes and conservation
23 practices, *Agriculture, Ecosystems and Environment*, 128(4), 225–238, 2008.
- 24 Williams, G. P.: Sediment concentration versus water discharge during single hydrologic
25 events in rivers, *Journal of Hydrology*, 111, 89–106, 1989.
- 26 Zech, W., Senesi, N., Guggenberger, G., Kaiser, K., Lehmann, J., Miano, T.M., Miltner, A.
27 and Schroth, G.: Factors controlling humification and mineralization of soil organic matter in
28 the tropics, *Geoderma*, 79, 117–161, 1997.

Table 1. Mean organic matter composition and ^{137}Cs activity (± 1 standard deviation) for surface soils (n=64), gullies (n=5) and stream bank (n=6) samples in the Houay Pano and Houay Xon catchments. For ^{137}Cs activity measurements, see Gourdin et al. (2014).

Location	TOC (mgC g ⁻¹)	TN (mgN g ⁻¹)	TOC/TN	$\delta^{13}\text{C}$ (‰)	$\delta^{15}\text{N}$ (‰)	^{137}Cs (Bq kg ⁻¹)
Surface soils*	25 ± 5	2.1 ± 0.5	11.6 ± 2.0	-25.5 ± 1.4	6.7 ± 1.3	2.2 ± 0.9
Stream banks**	13 ± 6	1.1 ± 0.3	12.4 ± 7.7	-23.2 ± 4.4	8.6 ± 1.9	0.4 ± 0.3
Gullies**	14 ± 7	1.4 ± 0.6	9.6 ± 0.8	-22.7 ± 0.8	8.7 ± 2.1	0.4 ± 0.3

*Data from Huon et al. (2013) and this study (2012), **this study (2012).

Table 2. Estimates of event water discharge (EWD) and related specific runoff (SR) and runoff coefficient (RC) for the three stations during the 23 May 2012 flood.

Station	Drainage area (km ²)	EWD* (x 10 ⁶ L)	SR** (mm)	RC*** (%)
S1	0.2	0.215	1.1	4.0
S4	0.6	1.88	3.2	11.7
S10	11.6	12.2	1.1	3.9

* EWD = total water discharge minus baseflow discharge

** SR = EWD / drainage area

*** RC = 100 x (SR / rainfall) assuming an homogeneous cumulative rainfall of 27 mm

Table 3. Total suspended sediment yield (SSY), total particulate organic carbon yield (C_{SSY}), specific total suspended sediment yield (S_Y) and specific total organic carbon yield (C_Y) for the 23 May 2012 flood.

Station	SSY (Mg)	C _{SSY} (kg)	S _Y * (kg ha ⁻¹)	C _Y ** (kgC ha ⁻¹)
S1	2.3	58	115	2.9
S4	26	496	433	8.3
S10	130	4346	112	3.7

* S_y = 10 x SSY / drainage area in Table 2

** C_Y = 10⁻² x C_{SSY} / drainage area in Table 2

Appendix A: Table A1. Summary of data for stations S1, S4 and S10 during the 23 May 2012 flood.

Label	Time*	TSS*	Q*	EC*	$\delta^{18}\text{O}^*$	TOC*	TN*	TOC/TN*	$\delta^{13}\text{C}^*$	$\delta^{15}\text{N}^*$
	(hh:mm)	(g L ⁻¹)	(L s ⁻¹)	($\mu\text{S cm}^{-1}$)	(‰ vs. V-SMOW)	(mgC g ⁻¹)	(mgN g ⁻¹)		(‰ vs. PDB)	(‰ vs. AIR)
Station S1										
LS0101	12:08	0.86	5	335	-7.2	42.0	2.0	20.5	-15.3	7.1
LS0102	12:09	0.56	7	317	-7.1	60.3	2.6	23.1	-19.0	5.5
LS0103	12:09	0.53	10	317	-7.0	-	-	-	-	-
LS0104	12:10	0.61	13	299	-6.8	66.2	2.1	31.0	-19.7	7.0
LS0105	12:10	-	16	299	-	-	-	-	-	-
LS0106	12:11	1.23	21	282	-6.9	32.2	2.3	14.0	-23.0	6.0
LS0107	12:13	1.70	27	262	-6.6	26.2	2.0	13.0	-23.7	6.6
LS0108	12:14	2.37	34	259	-6.2	25.0	2.0	12.7	-22.4	6.8
LS0109	12:19	3.65	40	241	-6.0	23.1	2.1	10.8	-24.4	7.2
LS0110	12:20	4.17	55	233	-6.1	23.4	2.2	10.7	-24.5	7.3
LS0111	12:21	4.65	76	224	-5.9	22.5	2.0	11.1	-24.1	7.5
LS0112	12:21	18.74	90	215	-5.8	27.4	2.0	11.1	-25.6	6.8
LS0113	12:30	29.98	68	184	-5.8	25.7	2.1	11.0	-25.8	6.8
LS0114	12:33	23.02	51	188	-5.5	25.8	2.2	10.7	-25.9	7.5
LS0115	12:37	24.05	38	194	-5.4	23.3	2.0	10.1	-25.8	7.5
LS0116	12:43	17.67	27	205	-5.6	20.8	2.5	9.8	-25.6	7.7
LS0117	12:50	16.38	18	218	-5.7	19.3	2.3	9.0	-25.3	7.8
LS0118	12:57	9.13	14	232	-5.8	18.7	2.4	9.0	-25.0	7.5
LS0119	12:58	14.37	13	233	-6.1	18.6	2.3	9.1	-25.1	7.2
LS0120	13:15	4.50	8	262	-6.2	19.3	2.1	9.6	-23.8	7.1
Station S4										
LS0403	11:57	1.53	15	297	-6.9	-	-	-	-	-
LS0404	11:58	1.21	24	306	-6.7	-	-	-	-	-
LS0403-4**	-	-	-	-	-	27.7	2.6	10.8	-23.8	7.1
LS0405	12:00	1.16	33	306	-6.5	29.9	2.9	10.4	-23.5	6.5
LS0406	12:01	2.71	42	262	-6.1	24.8	2.4	10.2	-24.4	7.2
LS0407	12:04	5.83	54	216	-5.5	22.6	2.2	10.5	-25.0	7.2
LS0408	12:05	6.83	76	205	-5.2	-	-	-	-	-
LS0409	12:06	7.25	114	198	-5.3	-	-	-	-	-
LS0408-9**	-	-	-	-	-	21.2	2.1	10.1	-25.0	7.5
LS0410	12:07	10.07	144	177	-4.7	22.1	2.1	10.7	-25.2	7.6
LS0411	12:07	11.89	185	161	-4.7	20.8	2.0	10.3	-25.2	7.6
LS0412	12:08	15.75	280	138	-4.5	19.2	1.9	9.9	-25.6	7.6
LS0413	12:09	20.05	309	121	-4.9	-	-	-	-	-
LS0414	12:10	31.56	358	99	-5.1	19.6	2.1	9.6	-25.4	8.0
LS0415	12:11	46.51	440	87	-5.2	21.1	2.1	10.0	-25.6	7.5

Label	Time*	TSS*	Q*	EC*	$\delta^{18}\text{O}^*$	TOC*	TN*	TOC/TN*	$\delta^{13}\text{C}^*$	$\delta^{15}\text{N}^*$
	(hh:mm)	(g L ⁻¹)	(L s ⁻¹)	($\mu\text{S cm}^{-1}$)	(‰ vs. V-SMOW)	(mgC g ⁻¹)	(mgN g ⁻¹)		(‰ vs. PDB)	(‰ vs. AIR)
LS0416	12:20	28.40	335	103	-5.4	24.5	2.1	11.5	-26.0	7.1
LS0417	12:23	23.00	277	105	-5.4	24.7	2.2	11.4	-25.8	7.2
LS0418	12:26	17.76	228	117	-5.6	24.7	2.1	11.8	-26.0	7.4
LS0419	12:34	11.70	183	152	-5.6	-	-	-	-	-
LS0420	13:20	12.62	145	164	-5.6	-	-	-	-	-
LS0419-20**	-	-	-	-	-	22.5	2.0	11.0	-25.8	7.4
LS0421	13:32	7.71	112	192	-5.8	19.0	1.9	9.8	-25.6	7.7
LS0422	13:46	6.92	84	201	-6.1	19.6	2.0	9.8	-25.6	7.7
LS0423	14:05	6.93	59	203	-6.0	-	-	-	-	-
LS0424	14:43	5.89	39	214	-6.2	-	-	-	-	-
LS0425	15:46	3.37	23	230	-6.2	-	-	-	-	-
LS0423-25**	-	-	-	-	-	20.9	2.2	9.6	-25.5	7.3
Station S10										
LS1002	12:24	7.94	204	227	-5.5	-	-	-	-	-
LS1003	12:28	5.57	455	220	-5.5	-	-	-	-	-
LS1002-3**	-	-	-	-	-	39	2.0	19.8	-21.2	8.2
LS1004	12:31	8.77	623	215	-5.9	-	-	-	-	-
LS1005	13:03	11.10	943	167.5	-5.6	-	-	-	-	-
LS1004-5**	-	-	-	-	-	36	1.9	19.1	-22.6	7.4
LS1006	13:06	23.63	990	167	-5.7	44	1.9	23.1	-21.8	7.0
LS1007	13:27	17.02	1535	156	-5.4	44	2.0	22.2	-22.3	7.5
LS1008	13:33	24.43	1350	155.5	-5.7	29	1.8	16.2	-22.7	8.4
LS1009	13:39	24.00	1187	157	-5.6	31	1.8	17.2	-23.0	7.9
LS1010	13:46	15.74	1038	160	-5.6	25	1.8	13.7	-24.3	7.9
LS1011	13:55	21.47	886	167.5	-5.7	27	1.9	14.3	-23.4	7.3
LS1012	14:06	18.01	735	174	-5.6	29	1.9	15.0	-24.5	7.4
LS1013	14:20	15.35	597	184	-5.8	24	2.0	12.4	-24.5	7.1
LS1014	14:38	12.80	485	198	-5.7	-	-	-	-	-
LS1015	15:14	10.17	308	222	-5.9	-	-	-	-	-
LS1014-15**	-	-	-	-	-	30	1.9	15.5	-23.6	7.1

* = Time of collection, total suspended sediment load (TSS), stream discharge (Q), water electric conductivity (EC) and $\delta^{18}\text{O}$, total organic carbon in TSS (TOC), total nitrogen in TSS (TN), $\delta^{13}\text{C}$ and $\delta^{15}\text{N}$ for TSS, ** = composite sample, - = no value.

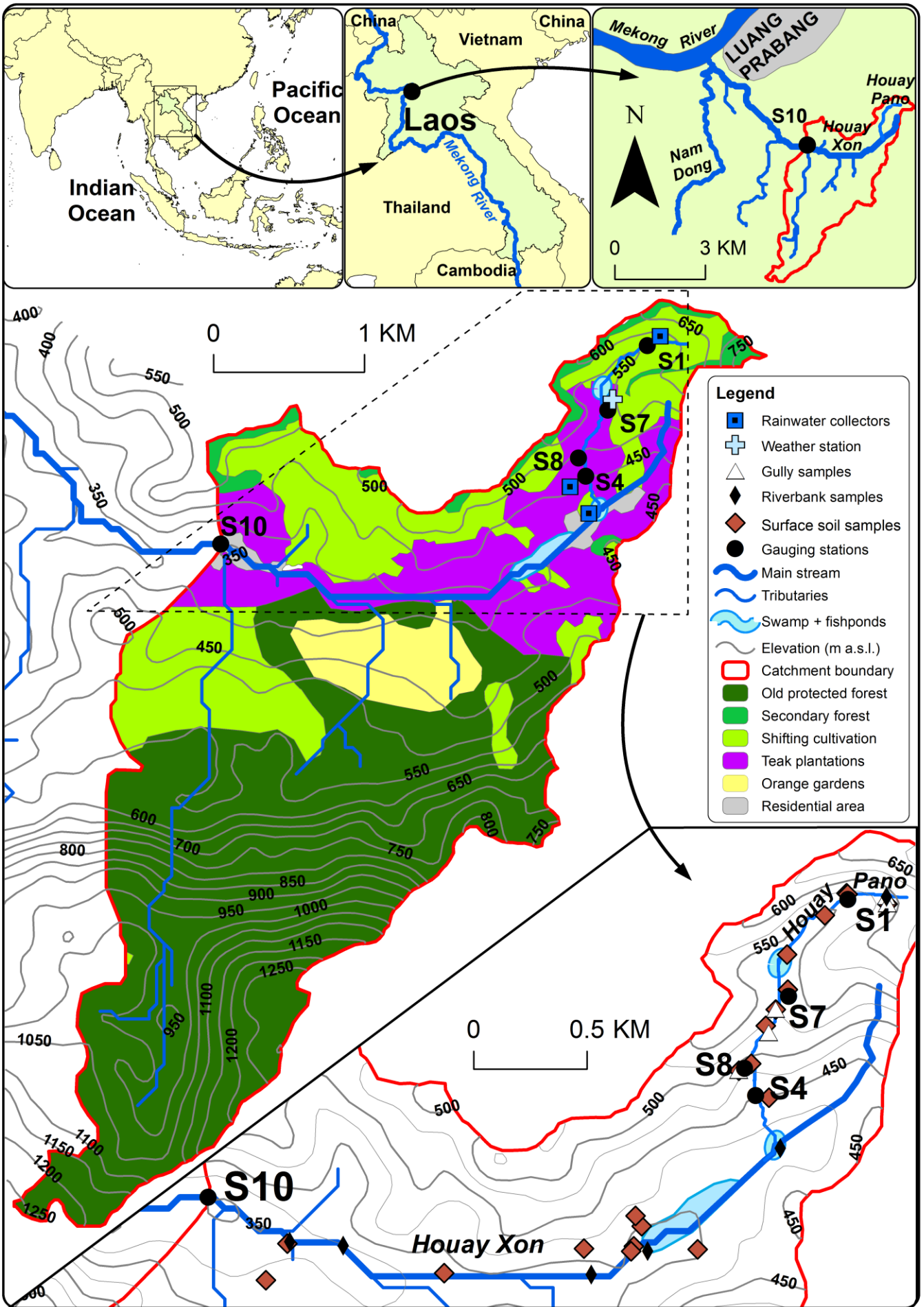


Fig. 1. Location of the Houay Xon River catchment in SE Asia (a). Topographic and land use map of the Houay Xon S10 sub-catchment in 2012 with location of the gauging stations (S1, S4, S7, S8, S10), rainwater collectors and automatic weather station (b), surface soil, gully and riverbank sampling locations (c).

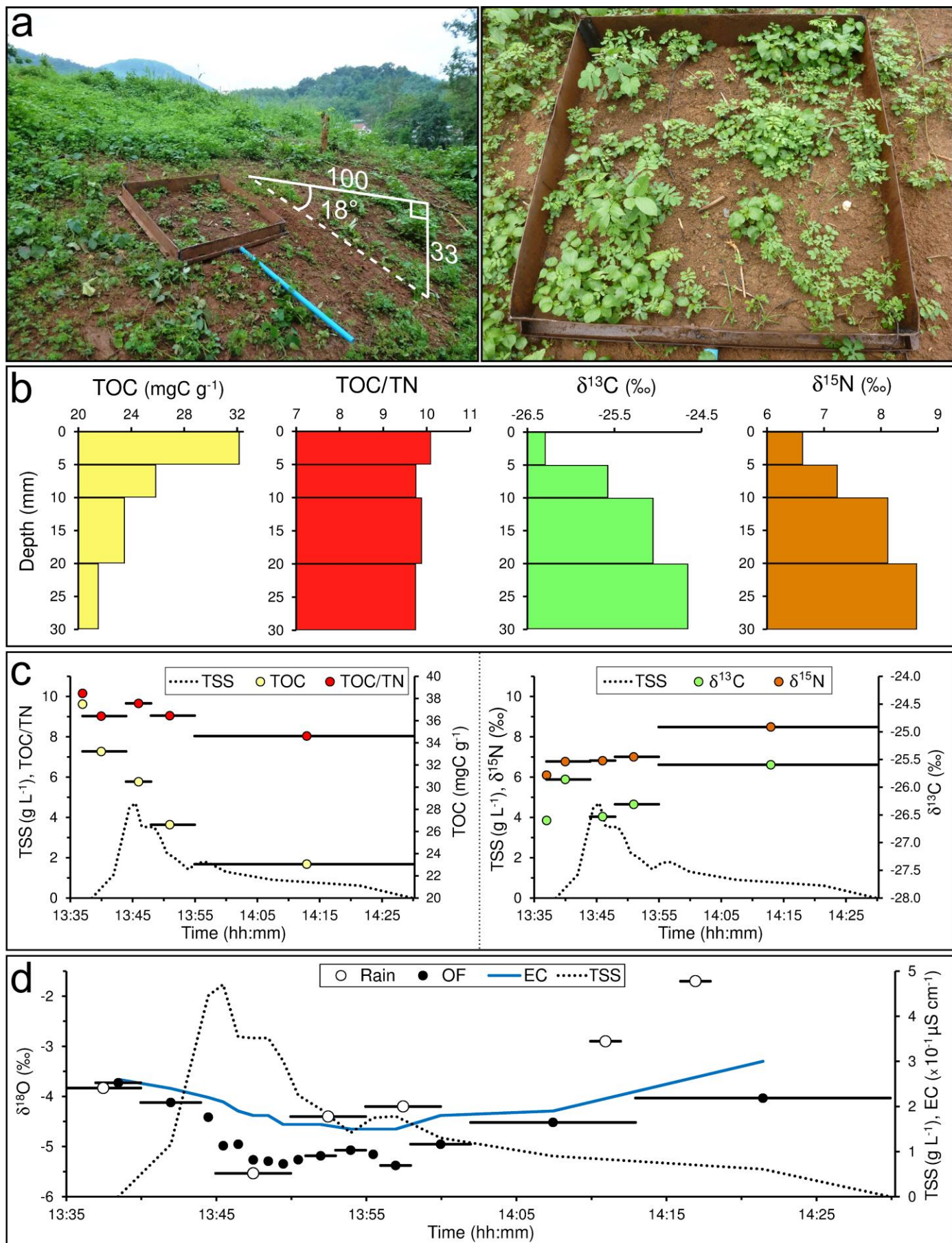


Fig. 2. Microplot experiment: (a) presentation of the 1-m² collecting system and its vegetation cover; (b) Distribution of topsoil total organic carbon (TOC) concentration, total organic carbon : total nitrogen ratio (TOC/TN), $\delta^{13}\text{C}$ and $\delta^{15}\text{N}$ with soil depth; (c) temporal evolution of the total suspended sediment load (TSS) plotted with TOC and TOC/TN in TSS (left) and with $\delta^{13}\text{C}$ and $\delta^{15}\text{N}$ in TSS (right) during the June 1st storm and (d) temporal evolution of the overland flow TSS load with rainwater- $\delta^{18}\text{O}$ (Rain), overland flow- $\delta^{18}\text{O}$ (OF) and overland flow electric conductivity (EC) during the June 1st storm.

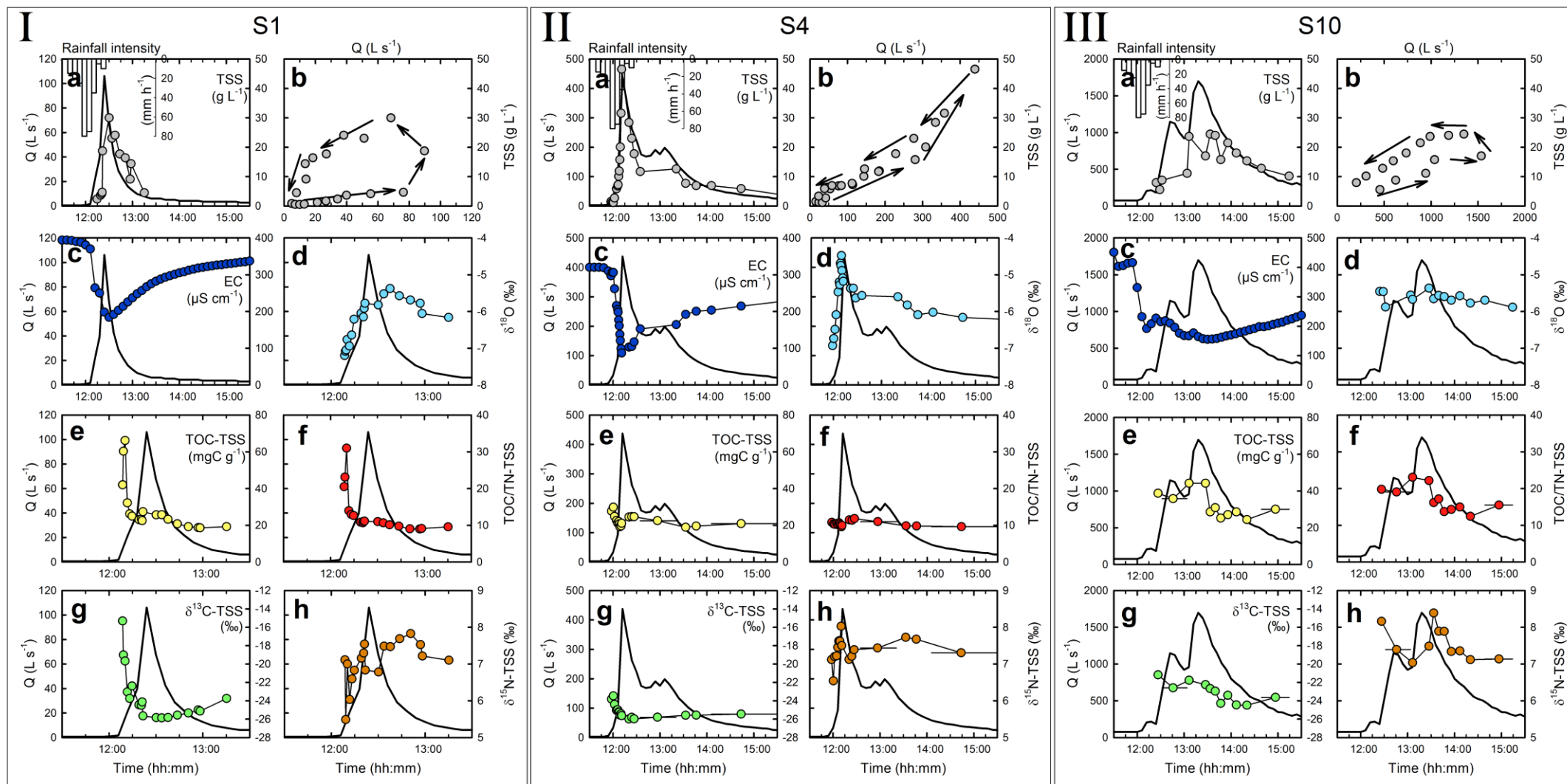


Fig. 3. Plots of the temporal evolution of (a) rainfall intensity, stream discharge (Q , thicker solid line), (b) total suspended sediment load (TSS), (c) water electric conductivity (EC), (d) streamwater- $\delta^{18}\text{O}$, (e) total organic carbon concentration in the TSS (TOC-TSS), (f) total organic carbon : total nitrogen ratio in the TSS (TOC/TN-TSS), (g) $\delta^{13}\text{C}$ -TSS, (h) $\delta^{15}\text{N}$ -TSS for : (I) the upstream station S1, (II) the intermediate station S4, and (III) the downstream station S10, during the 23 May 2012 flood. Horizontal bars represent sampling period for composite samples.

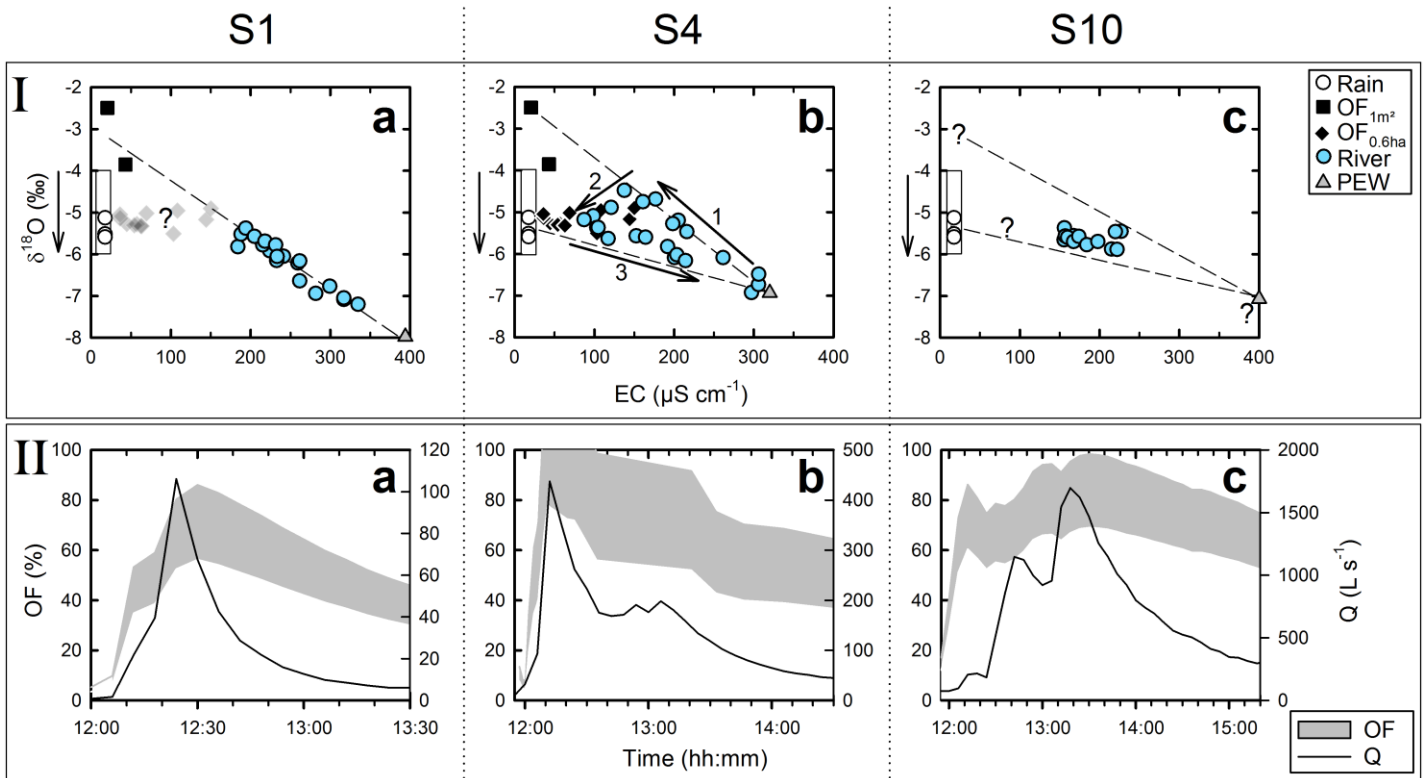


Fig. 4. Plots of: (I) relationships between water electric conductivity (EC) and water $\delta^{18}\text{O}$, and (II) temporal evolution of stream water discharge (Q) with overland flow contribution estimates (OF) for (a) the upstream station S1, (b) the intermediate station S4, and (c) the downstream station S10, during the 23 May 2012 flood. In (I), open circles correspond to rainwater, filled squares to cumulative overland flow obtained with 1- m^2 plots (OF_{1m^2}), filled diamonds to overland flow from S7 and S8 hillslopes ($\text{OF}_{0.6\text{ha}}$), filled colored circles to stream water, triangles to pre-event water (PEW). The rectangle areas and vertical arrows represent the potential temporal variability of rainwater- $\delta^{18}\text{O}$ during the storm. In (II), the shaded area corresponds to the variability range for the estimated overland flow contribution.

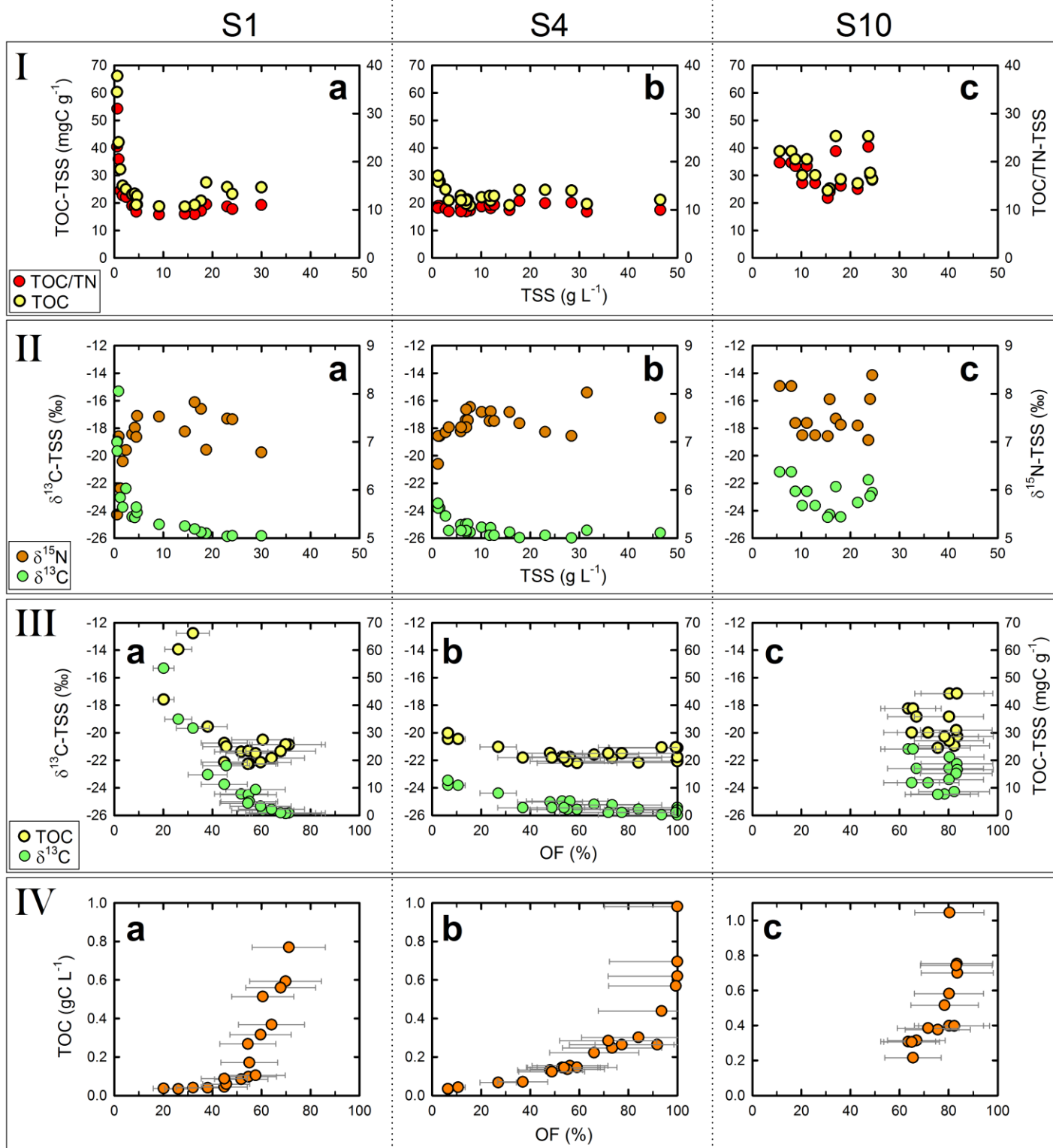


Fig. 5. Relationships between total suspended sediment load (TSS), total organic carbon concentration in the TSS (TOC-TSS), total organic carbon : total nitrogen ratio in the TSS (TOC/TN-TSS), $\delta^{13}\text{C}$ -TSS, $\delta^{15}\text{N}$ -TSS, total organic carbon load (TOC) and overland flow contribution estimates (OF): (a) at upstream station S1 (Houay Pano Stream), (b) at intermediate station S4, and (c) at downstream station S10, during the 23 May 2012 flood. In (III) and (IV), circles represent the median values of the variability range (horizontal bars) of estimated OF contribution.

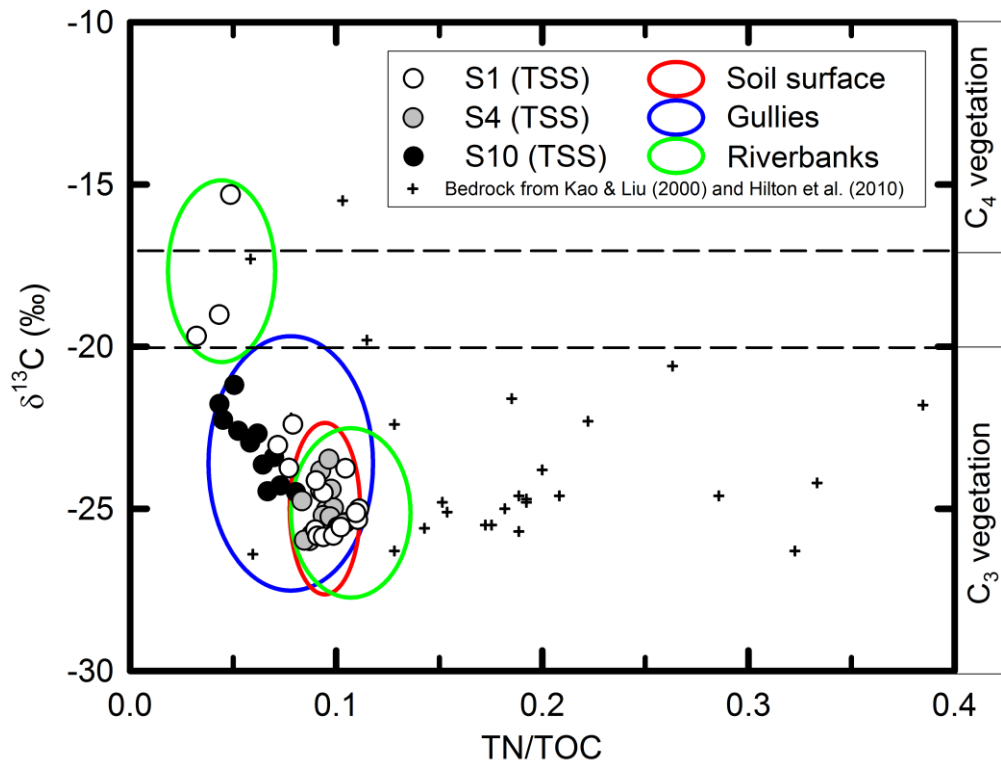


Fig. 6. Plot of $\delta^{13}\text{C}$ vs. TN/TOC for total suspended sediment loads (TSS) collected at S1 (open circles), S4 (grey circles) and S10 (closed circles) during the 23 May 2012 flood and for the potential sources of sediment (Soil surface: red area; Gullies: blue area; Riverbanks: green areas) determined in the catchment. Bedrock data (plus signs) are taken from literature (Kao and Liu, 2000; Hilton et al., 2010).